Nonclinical Efficacy and Safety of CX-2029, an Anti-CD71 Probody–Drug Conjugate

Shweta Singh[1], Laura Serwer[1], Amy DuPage[1], Kristi Elkins[1], Niharika Chauhan[2], Matthew Ravn[2], Fritz Buchanan[2], Leyu Wang[2], Michael Krimm[1], Ken Wong[1], Jason Sagert[1], Kimberly Tipton[1], Stephen J. Moore[1], Yuanhui Huang[1], Andrew Jang[1], Eric Ureno[1], Adam Miller[1], Sarah Patrick[1], Shanti Duvur[1], Shouchun Liu[1], Olga Vasiljeva[1], Yingchun Li[2], Tracy Henriques[2], Ilaria Badagnani[2], Shawn Jeffries[2], Siew Schleyer[1], Rob Leanna[2], Claus Krebber[1], Sridhar Viswanathan[1], Luc Desnoyers[1], Jonathan Terrett[1], Marcia Belvin[1], Susan Morgan-Lappe[2], W. Michael Kavanaugh[1], and Jennifer Richardson[1]

ABSTRACT

Probody therapeutics (Pb-Txs) are conditionally activated antibody–drug conjugates (ADCs) designed to remain inactive until proteolytically activated in the tumor microenvironment, enabling safer targeting of antigens expressed in both tumor and normal tissue. Previous attempts to target CD71, a highly expressed tumor antigen, have failed to establish an acceptable therapeutic window due to widespread normal tissue expression. This study evaluated whether a probody–drug conjugate targeting CD71 can demonstrate a favorable efficacy and tolerability profile in preclinical studies for the treatment of cancer. CX-2029, a Pb-Tx conjugated to maleimido-caproyl-valine-citrulline-p-aminobenzyloxycarbonyl-monomethyl auristatin E, was developed as a novel cancer therapeutic targeting CD71. Preclinical studies were performed to evaluate the efficacy and safety of this anti-CD71 PDC in patient-derived xenograft (PDX) mouse models and cynomolgus monkeys, respectively. CD71 expression was detected at high levels by IHC across a broad range of tumor and normal tissues. *In vitro*, the masked Pb-Tx form of the anti-CD71 PDC displayed a >50-fold reduced affinity for binding to CD71 on cells compared with protease-activated, unmasked anti-CD71 PDC. Potent *in vivo* tumor growth inhibition (stasis or regression) was observed in >80% of PDX models (28/34) at 3 or 6 mg/kg. Anti-CD71 PDC remained mostly masked (>80%) in circulation throughout dosing in cynomolgus monkeys at 2, 6, and 12 mg/kg and displayed a 10-fold improvement in tolerability compared with an anti-CD71 ADC, which was lethal. Preclinically, anti-CD71 PDC exhibits a highly efficacious and acceptable safety profile that demonstrates the utility of the Pb-Tx platform to target CD71, an otherwise undruggable target. These data support further clinical development of the anti-CD71 PDC CX-2029 as a novel cancer therapeutic.

Introduction

In recent years, antibody–drug conjugates (ADCs) have emerged as attractive options for the treatment of patients with cancer. As of this writing, nine ADCs have received U.S. FDA approval for a variety of hematopoietic and solid tumors, and more than 80 ADCs are currently under evaluation in clinical trials (1, 2).

ADCs comprise three components: an mAb directed to a tumor antigen, a cytotoxic payload, and a cleavable or noncleavable linker that joins the first two components (3). Upon binding of an ADC to its target antigen, the ADC is internalized, and the payload is released intracellularly to mediate its cytotoxic effects (4). The payload of an ADC, typically a chemotherapeutic agent that inhibits microtubule assembly or disrupts DNA, is usually extremely potent with a narrow therapeutic window such that these agents cannot be used as free drugs. The efficacy and safety of an ADC depends on the potency of the payload and the ability of the antibody to specifically target high antigen-expressing tumor cells with a suitable therapeutic window (5).

Candidate ADC targets must be carefully selected with attention to numerous properties that can influence efficacy and safety. ADCs have shown their greatest clinical utility when targeting antigens that are expressed at high levels on cancer cells (6) with minimal target expression in normal tissue (7). Furthermore, antibody binding to the target antigen must lead to rapid effective internalization and lysosomal targeting (3). Given these requirements for ADC approaches, identifying candidate targets can be challenging.

CD71, also known as transferrin receptor 1 (TfR1), is involved in the cellular uptake of iron and is expressed at high levels on rapidly proliferating cells, such as cancer cells (8). Upon internalization and trafficking to the low pH endosome where iron is released, CD71 recycles back to the cell surface. These features enable efficient delivery of cytotoxin into the cell with a CD71-targeted ADC. Many cancers that are sensitive to microtubule inhibitor (MTI) drugs, such as esophageal, non-Hodgkin's lymphoma [NHL; mostly diffuse large B-cell lymphoma (DLBCL)], breast, lung, ovarian, and endometrial cancers, have a prevalence of high CD71 expression and may represent indications that would respond to a CD71-targeted MTI (9–12). The development of a CD71-targeted ADC has been limited by safety challenges (13), resulting in on-target toxicity in normal tissues, leading to the notion that CD71 may represent an "undruggable" ADC target.

Probody therapeutics have recently been developed as a novel approach to target attractive tumor antigens that are difficult-to-treat due to high or widespread tissue expression (14, 15). These recombinant, proteolytically activatable antibody prodrugs contain an anticancer monoclonal IgG antibody, a masking peptide linked to the N-terminus of the light chain and a protease-cleavable substrate linker peptide (16, 17). Although the Probody therapeutic remains mainly intact and masked and thus blocked from target binding in normal tissue, the presence of tumor-specific protease activity results in "un-masking" to allow binding of the antibody to the target within the tumor. Probody therapeutics can potentially improve the therapeutic window for validated targets and create a therapeutic window for difficult-to-drug targets. The Probody therapeutic approach can be applied to safely target numerous antibody-based therapies, including ADC approaches. Thus, a Probody–drug conjugate (PDC) approach allows enhanced tumor-specific binding of the ADC, potentially facilitating improved efficacy and safety over the ADC approach.

The PDC approach overcomes a key limitation of traditional ADCs, which is a requirement for low expression of the target in normal tissues. Because of their restricted potential for target engagement outside the tumor environment, moderate to high target expression in normal tissue can be acceptable for PDCs. Therefore, PDCs can enable targeting of tumor antigens whose normal tissue expression presents a barrier to the development of conventional ADCs. Preliminary results of PDC clinical evaluation have shown early signs of efficacy and encouraging safety profiles (18).

To assess whether the PDC approach can be applied as a novel therapeutic strategy to target CD71, CX-2029, a monomethyl auristatin E (MMAE)-conjugated PDC with a purified drug-to-Probody ratio (DPR) of 2, was developed. MMAE is an antimitotic agent that causes metaphase arrest of dividing cells, resulting in cell death (4). Normal noncancerous tissues are expected to be spared from the cytotoxic effects of this anti-CD71 PDC due to impaired binding to CD71. In contrast, high-affinity binding of the activated anti-CD71 PDC to CD71 in a protease-rich tumor microenvironment (TME) should result in potent cytotoxic activity in cancer tissues. High expression of CD71 across numerous types of cancers suggests that an anti-CD71 PDC may be particularly effective as a cancer therapeutic. The objective of this study was to assess the therapeutic potential of the anti-CD71 PDC CX-2029 for the treatment of cancer by evaluating its efficacy and safety in preclinical models.

Materials and Methods

Animal studies

All animal studies were executed in compliance with institutional guidelines and regulations and after approval from the appropriate Institutional Animal Care and Use Committees. Mouse xenograft studies were performed by Champions Oncology, Crown Biosciences, or CytomX Therapeutics, and cynomolgus monkey studies were performed by Charles River Laboratories. All animal studies followed regulations set forth by the USDA Animal Welfare Act and the Guide for the Care and Use of Laboratory Animals.

Test articles

Test article descriptions are provided in Supplementary Table S1. CX-051 is a humanized IgG1 kappa mAb to CD71-derived from a mouse hybridoma generated by immunizing mice with the extracellular domain (ECD) of the CD71 protein.

CX-2014 and CX-2030 are anti-CD71 ADCs composed of CX-051 conjugated to maleimido-caproyl-valine-citrulline-p-aminobenzyloxycarbonyl-monomethyl auristatin E (vcMMAE) with a DAR of nearly 3.5 or 2, respectively.

CX-151 is a protease-activatable antibody prodrug (Probody protein) derived from CX-051. The two light chains in CX-151 are N-terminally extended to include a 47-amino acid prodomain, which serves to mask the target binding region of the antibody. The primary amino acid sequences for the CX-151 heavy chain and the modified light chain are available in the published US patent publication as SEQ ID No. 167 and SEQ ID No. 20, respectively (19). Both coding sequences were synthesized *de novo*, inserted into a CHO expression vector, transfected into a CHO cell line to establish stable pools from which a clone was selected for cell bank generation. CX-151 was produced in a culture and purified.

CX-2029 is an anti-CD71 PDC composed of CX-151 conjugated to vcMMAE. Partially reduced CX-151 was conjugated via its free thiols to vcMMAE, then highly enriched by Butyl Sepharose HP hydrophobic interaction chromatography for PDC species with a DPR of ∼2 (E2; Supplementary Fig. S1; Supplementary Table S2). High purity was achieved for CX-2029 with aggregate levels less than 1% (by SEC-HPLC), unmasked CX-2029 levels less than 1% (by reduced CE-SDS), and an overall DPR of 1.9.

CD71 IHC

IHC for CD71 was performed using formalin-fixed paraffin-embedded tissue microarrays for human multiple organ normal tissue, primary tumor tissues, and metastatic disease (US Biomax) or patient-derived xenograft (PDX) microarrays from Champions Oncology. Microarrays for primary and metastatic tumor tissues included samples from esophageal cancer, gastric cancer, pancreatic cancer, NHL, lung cancer, breast cancer, colorectal cancer, and head and neck squamous cell carcinoma (HNSCC). IHC was performed using the D7G9X rabbit mAb directed against the ECD of CD71 (Catalog No. 13113; Cell Signaling Technology) and a biotinylated donkey anti-rabbit secondary and an avidin-biotin complex HRP detection system. Placenta and prostate tissue were included as positive and negative controls, respectively. Standard IHC protocols were used (Supplementary Materials and Methods).

In vitro cytotoxicity

Human tumor cell lines representing 10 cancer types were purchased from ATCC, European Collection of Authenticated Cell Cultures (ECACC) or Leibniz Institute DSMZ-German Collection of Microorganisms and Cell Cultures and grown in complete media of RPMI supplemented with 10% FBS or according to the manufacturer's recommendations. No additional authentication of cell lines or mycoplasma testing was performed after purchase. Cells were propagated according to the manufacturer's guidelines, generating working cell banks of up to no more than passage 3 to 5. Working cell banks were stored in liquid nitrogen and, upon thaw, propagated for no more than 10 to 15 additional passages. Suspension or adherent cells were plated at a density of 1,000 cells/well in 50-μL complete media in a 96-well white-walled tissue culture plate and used immediately or allowed to adhere overnight. Cells were then incubated with 50 μL of a 2× final concentration of test article for 3 to 5 days at 37°C and 5% CO_2. Cell Titer Glo reagent (Promega) was then added to each well, and luminescence (RLU) was measured on a SpectraMax M5 plate reader (Molecular Devices). Duplicate wells were tested for each condition, and data were graphed as a percent of control in GraphPad Prism (GraphPad Software). Data were expressed as % control = (mean RLU test article/mean RLU untreated control) × 100, where untreated control consists of cells incubated in complete media without any test

article. Data were analyzed by nonlinear regression, and EC_{50} values were determined using a four-parameter logistic curve fit, where EC_{50} is the concentration of test article that gives half-maximal response.

Indirect binding ELISA

Indirect ELISA was performed using recombinant human CD71 (rhCD71, R&D systems or made in-house) or recombinant cynomolgus CD71 (rcCD71, Sino Biologicals). Briefly, 96-well high-binding plates were coated with 200 ng/well of rhCD71 ECD protein or rcCD71 ECD protein overnight at 4°C. Plates were washed, blocked with PBS + 0.5% BSA, washed again, then incubated in 100 μL of indicated concentrations of test article or isotype ADC in block buffer for 1 hour at room temperature. Plates were then washed again and incubated in 100 μL of detection antibody (Peroxidase AffiniPure anti-human IgG, Jackson ImmunoResearch) at a 1:25,000 dilution in block buffer for 1 hour at room temperature. After washing, plates were incubated with 100 μL/well of 1-Step Ultra TMB ELISA Substrate (Thermo Fisher Scientific) for 10 minutes at room temperature, followed by 100 μL/well of 1 M hydrochloric acid to stop the reaction. Absorbance was then measured on a SpectraMax plate reader (Molecular Devices) and reported as optical density (OD) at 450 nm. Data were graphed in Graphpad Prism (Grahpad Software), and apparent equilibrium binding constants (Kapp) were determined using nonlinear regression four parameter logistic (4-PL) analysis. Full method details as well as methods for direct binding ELISAs can be found in Supplementary Materials and Methods.

For protease activation, anti-CD71 PDC was diluted to 1 mg/mL in PBS and incubated with 10% volume of matriptase (R&D Systems, No. 3946-SE; 0.25 mg/mL) or PBS for approximately 4 to 5 hours at 37°C. Reactions were performed in a final volume of 200 to 300 μL. Confirmation of cleavage was assessed by SDS-PAGE.

Cell binding assays

HCC1806 cells were obtained from ATCC and grown in complete media. CHO-K1 cells expressing cynomolgus monkey CD71 cells were generated at AbbVie and grown in Hybridoma SFM + L-glutamine media supplemented with 1% FBS, 1 mmol/L HEPES, Pen-Strep, and 2 mg/mL Geneticin. Cells were harvested using Versene cell dissociation buffer and washed with PBS pH 7.2 + 0.5% BSA. Cells were incubated with the indicated concentrations of test article in PBS + 0.5% BSA for 1 hour on ice. After washing 3× with PBS + 0.5% BSA, cells were incubated with a goat anti-human IgG secondary antibody conjugated to Alexa Fluor 647 (Jackson ImmunoResearch, Catalog No. 109–605–098) for 45 minutes on ice. Cells were then washed 3× with PBS + 0.5% BSA and fixed with 1% formaldehyde. Bound antibody was detected using a Guava EasyCyte cytometer. Data were graphed in Graphpad Prism, and apparent equilibrium binding constants (Kapp) were determined using nonlinear regression 4-PL analysis.

In vivo efficacy studies

Female BALB/c nude mice used for esophageal, gastric, pancreatic models, and NOD/SCID, NPG, or NOG mice used for DLBCL models were sourced from Beijing Anikeeper Bio-Technology Co. Ltd. or Vital River, China, and used at ages 5 to 7 weeks. Seven- to 8-week-old female Athymic Nude-Foxn1nu mice were used for breast, HNSCC, and NSCLC models (Envigo). Human cancer cell lines or tumor fragments 2 to 3 mm in diameter from stock mice inoculated with primary human tumor xenografts were harvested and used to inoculate study mice by subcutaneous injection into the right flank. When tumors reached approximately 100 to 200 mm³, mice were randomized

into treatment groups based on tumor volume and body weight. Dosing started on the same day for all groups, and dosing volume was adjusted for each mouse based on body weight on day of dosing. PDX models were intravenously dosed with vehicle (PBS), 1.5 mg/kg, 3 mg/kg, or 6 mg anti-CD71 PDC on day 0 and day 7. Mice were checked daily for morbidity and mortality. Tumors were measured twice weekly via calipers.

Nonclinical safety studies

Groups of cynomolgus monkeys (6/sex/group) ranging from 2.4 to 2.7 years in age (2.1–3.7 kg) received intravenous (i.v.) bolus injections of vehicle or anti-CD71 PDC at 2, 6, or 12 mg/kg on day 1 (12 mg/kg) or days 1 and 22 (vehicle, 2 and 6 mg/kg). Scheduled animals were euthanized from 1 to 6 weeks after the last dose. In a separate study using cynomolgus monkeys 2.6 to 3.5 years in age (2.6–3.8 kg), anti-CD71 ADC was administered to a single animal at 2 mg/kg on day 1 and to one animal/sex at 0.6 mg/kg on days 1 and 22 with necropsy on day 29. Three animals were dosed with vehicle on days 1 and 22; necropsy was on day 29. Toxicity assessments for both studies included clinical observations, body weight, food consumption, clinical pathology, and anatomic pathology. Blood samples were collected throughout each study for toxicokinetic analysis. Additional details regarding bioanalytical methods for toxicokinetic analyses can be found in the Supplementary Materials and Methods.

Data availability statement

All data relevant to the study are included in the article or uploaded as online Supplementary Information. The datasets used and/or analyzed during this study are available from the corresponding author upon reasonable request.

Results

CD71 is highly expressed across multiple cancer types

To assess whether CD71 could serve as a potential PDC target for the treatment of cancer, CD71 cell surface expression was evaluated via IHC across a wide panel of tumor and normal tissue microarrays. Expression was evaluated in primary tumor and metastatic disease tissues from a variety of tumor types, including those with previously reported high levels of CD71 expression and responsiveness to MTIs. Moderate to strong CD71 expression was detected in most tissues tested, including from esophageal cancer, gastric cancer, pancreatic cancer, NHL, non–small cell lung cancer (NSCLC), breast cancer, and HNSCC (**Fig. 1A** and **B**; Supplementary Table S3).

We also examined CD71 expression in normal tissues. Among 27 human tissues examined, all samples contained CD71-expressing cells. Tissues with strong to moderate CD71 staining include adrenal gland, bone marrow, cerebrum, colon, esophagus, heart, kidney, liver, lung, nerve, small intestine, spleen, stomach, testis, thyroid, thymus, and uterus (**Fig. 1C**; Supplementary Tables S4 and S5).

Anti-CD71 ADC demonstrates potent in vitro cytotoxic activity across cancer cell lines

To confirm that targeting CD71 with an ADC approach could lead to antitumor effects, in vitro cytotoxicity assays were performed on a panel of 65 human cancer cell lines across 10 cancer types using an anti-CD71 antibody directly conjugated to MMAE. All cell lines tested displayed strong to moderate sensitivity to the CD71 ADC (**Fig. 2**). Among the cell lines tested, 8/8 gastric, 7/8 esophageal, 3/5 pancreatic, 7/8 CRC, 5/7 HNSCC, 2/6 small cell lung (SCLC), 6/7 NSCLC, 3/3 NHL, 6/7 triple-negative breast (TNBC), and 6/6 ER+ breast cancer
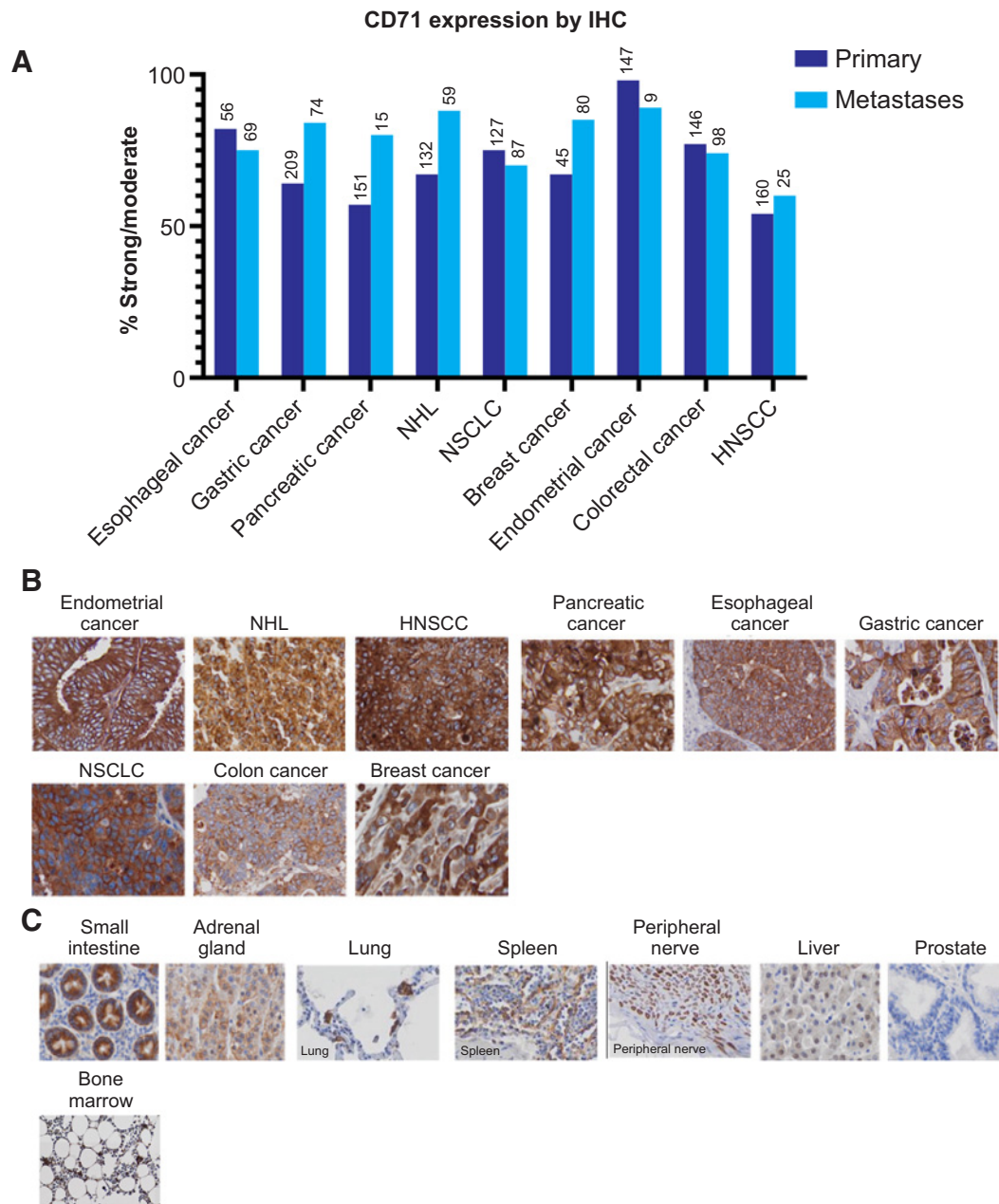
Figure 1.
CD71 is highly expressed across multiple cancer types. IHC for CD71 expression using a rabbit mAb directed against the ECD of CD71 revealed moderate to strong staining localized to the membrane and cytoplasm of all tumor types examined as well as the majority of normal tissues. **A,** Percentage of primary and metastatic samples on tumor microarrays with moderate to strong staining. Number of cores tested shown above bar graphs. **B** and **C,** Representative IHC images for tumor (**B**) and normal (**C**) tissues.

cell lines displayed EC_{50} values of ≤0.5 nmol/L (Supplementary Table S6).

Anti-CD71 PDC binding to human and cynomolgus CD71 is impaired by masking *in vitro*

Given the broad tumor expression and sensitivity of a wide variety of human cancer cell lines to an anti-CD71 ADC, development of a CD71-targeted PDC proceeded. The CX-2029 was designed as a CD71-targeting PDC composed of an anti-CD71

Probody therapeutic conjugated to the auristatin toxin MMAE via a valine-citrulline (vc) protease-cleavable linker with a DPR of 2 (E2 purified; **Fig. 3A**). In its intact prodrug form, this anti-CD71 PDC contains a prodomain composed of a mask that inhibits target binding and a protease-cleavable linker that can be cleaved by selected proteases, including the serine protease matriptase. Cleavage of the prodomain by proteases commonly activated in the tumor microenvironment releases the mask and yields the activated form of the anti-CD71 PDC. This design is intended to
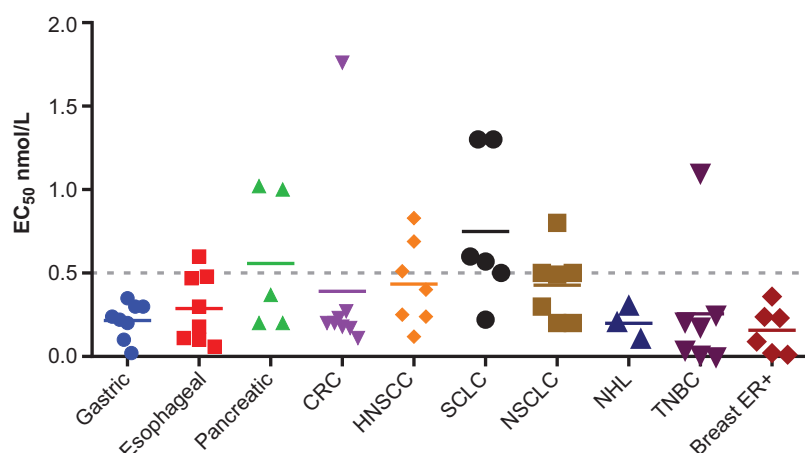
Figure 2.
CD71 ADC has potent subnanomolar EC_{50} cytotoxic activity across many human cancer cell lines *in vitro*. Human cancer cell lines were treated with increasing concentrations of the anti-CD71 ADC CX-2014 (anti-CD71-mc-vc-MMAE) for 3 to 5 days *in vitro*, and cell proliferation was measured using a Cell Titer Glo Proliferation Assay. Assays were performed in duplicate or triplicate, and median EC_{50} values were calculated for each cell line. The EC_{50} of a nonbinding matched isotype antibody conjugated to MMAE was not measurable within the range of the assay tested for many cell lines. Where measurable, EC_{50}s of the isotype control were ≥10-fold greater than the anti-CD71-vcMMAE activity.

minimize interaction of the anti-CD71 PDC with CD71 in normal tissues while effectively targeting CD71 in tumors.

To assess the binding capacity of the anti-CD71 PDC to CD71, ELISA and flow cytometry assays were performed to evaluate binding of intact or unmasked, activated anti-CD71 PDC to human and cynomolgus CD71. For these studies, the protease matriptase was used to activate the anti-CD71 PDC *in vitro* by cleaving the prodomain substrate linker peptide. The complete *in vitro* activation of the anti-CD71 PDC by matriptase was confirmed by SDS-PAGE.

Anti-CD71 PDC binding to recombinant human CD71 ECD protein (rhCD71) was evaluated by indirect ELISA (**Fig. 3B**, panel A; Supplementary Table S7). The binding activity of anti-CD71 PDC (CX-2029) was comparable with that of the unconjugated Probody therapeutic (CX-151), with apparent K_d (equilibrium dissociation constant; Kapp) values of 2.58 and 1.94 nmol/L, respectively. The binding activity of activated CX-151 (Kapp = 0.06 nmol/L) was similar to that of the unconjugated antibody (CX-051; Kapp = 0.03 nmol/L), demonstrating that vcMMAE conjugation did not alter antigen binding. Compared with the parental native antibody (CX-051), the masked Probody therapeutic protein (CX-151) and the anti-CD71 PDC (CX-2029) demonstrated an approximately 65-fold reduced affinity for binding to rhCD71. Protease cleavage of the anti-CD71 PDC prodomain restored binding activity (Kapp = 0.05 nmol/L) to a level comparable with that of the parental native antibody.

Binding of the anti-CD71 PDC to recombinant cynomolgus monkey CD71 (rcCD71) was also evaluated (**Fig. 3B**, panel B; Supplementary Table S7). The parental antibody bound to rcCD71 with a Kapp of 0.03 nmol/L. The activated form of the anti-CD71 PDC bound similarly with a Kapp of 0.04 nmol/L. In contrast, the "masked" form of the anti-CD71 PDC demonstrated a 26-fold reduced affinity for binding to rcCD71 (Kapp = 1.02 nmol/L).

The capacity of the anti-CD71 PDC to bind to CD71-expressing cells was evaluated by flow cytometry using human cancer cell lines, including HCC1806 human breast cancer, HT-29 human colorectal cancer, NCI-H292 human lung cancer, and NCI-H520 human lung cancer cell lines (**Fig. 3B**, panel C; Supplementary Table S7). The parental antibody bound to these cell lines with an affinity of approximately 1 nmol/L, and matriptase-activated anti-CD71 PDC bound with similar low affinities that ranged from 1.5 to 2.8 nmol/L. In contrast, the masked form of the anti-CD71 PDC showed an approximately 50-fold reduced binding affinity compared with the unmasked matriptase-activated form.

The ability of the anti-CD71 PDC to bind to cynomolgus monkey CD71 expressed on the cell surface was assessed using CHO K1 cells stably transfected with cynomolgus monkey CD71 (**Fig. 3B**, panel D; Supplementary Table S7). Flow cytometry indicated that the parental antibody bound to these cells with an affinity of 0.3 nmol/L, whereas the binding affinity of the anti-CD71 PDC was approximately 100-fold lower at 35 nmol/L. Matriptase activation led to increased binding of the anti-CD71 PDC with a Kapp value of 0.7 nmol/L.

Binding of the parental native antibody and protease-activated anti-CD71 PDC was comparable for human and monkey recombinant CD71 and within threefold on CD71-expressing cells. The Probody therapeutic peptide mask prevented binding of the PDC to CD71 in the absence of tumor-associated proteases. The data furthermore demonstrate the restoration of binding to CD71 upon protease activation of the PDC.

Protease-activated anti-CD71 PDC demonstrates *in vitro* cytotoxic activity

To assess the *in vitro* cytotoxic activity of the anti-CD71 PDC, HT29 and H520 cell lines were treated with increasing concentrations of the anti-CD71 PDC, matriptase-activated anti-CD71 PDC, or isotype control (Supplementary Fig. S2). In both cell lines, the anti-CD71 PDC and isotype control showed minimal cytotoxicity (EC_{50} values >50 nmol/L), whereas the matriptase-activated PDC demonstrated cytotoxicity with EC_{50} values of 1.3 and 1.2 nmol/L in HT29 and H520 cells, respectively, suggesting that protease activation substantially increases the cytotoxic effects of the PDC.

Anti-CD71 PDC competes with transferrin for binding to CD71

We next evaluated whether the humanized IgG1 monoclonal anti-CD71 antibody component of the anti-CD71 PDC competes with human holo-transferrin (hTf) for binding to CD71. This analysis used the parental antibody (CX-051) for the anti-CD71 PDC and a nonbinding isotype control antibody. Binding of hTf to recombinant human CD71 was evaluated by ELISA in the presence of the parental antibody (Supplementary Fig. S3). Biotinylated hTF (6 nmol/L) was incubated in the presence of increasing amounts of the parental antibody, and binding of hTf to plate-bound rhCD71 was measured following the addition of streptavidin-HRP. Compared with the isotype control antibody, increasing concentrations of the parental antibody led to a reduction of hTF binding, indicating a concentration-dependent blockade of hTf binding to rhCD71. However, the antibody did not compete as effectively as unlabeled hTf, which was included as
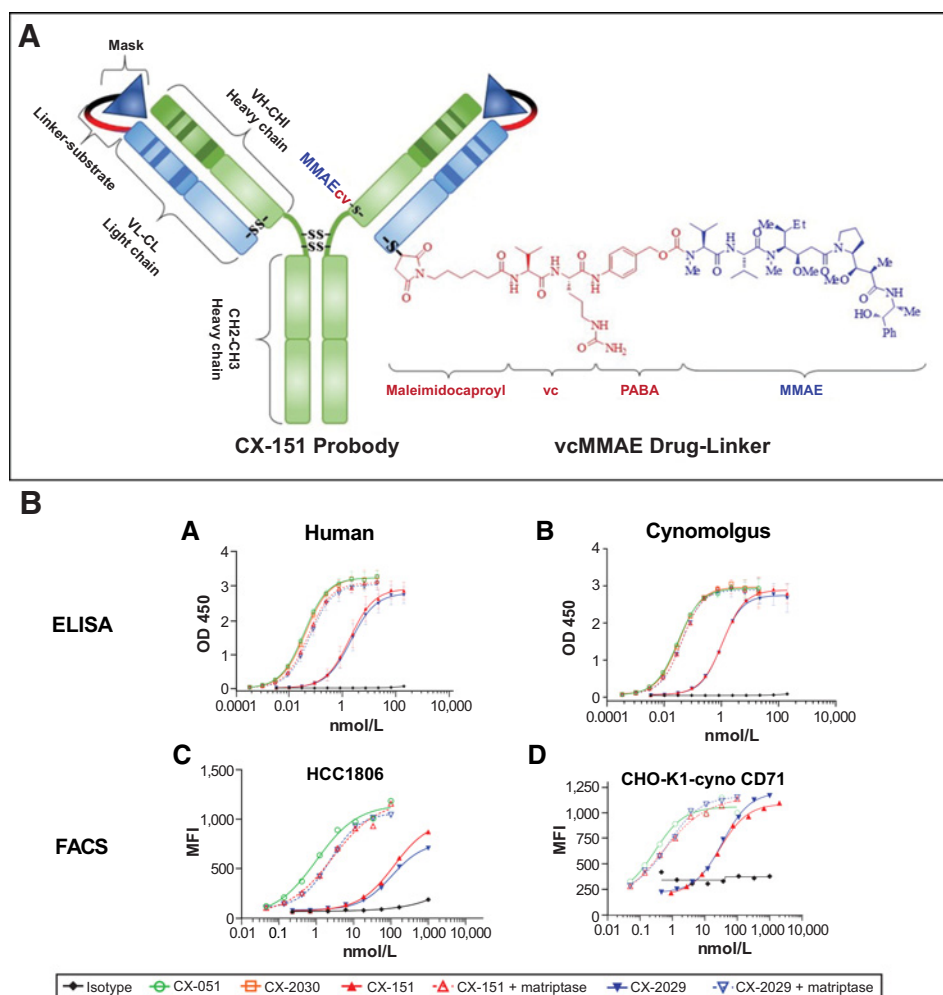
Figure 3.
Peptide mask impairs binding of anti-CD71 PDC (CX-2029) to CD71. **A,** Design of CX-2029, a PDC targeting CD71. CX-2029 comprises a humanized monoclonal IgG anti-CD71 Probody therapeutic (CX-151) conjugated to two molecules of -vc-MMAE (E2 purified; DPR = 2). The two vcMMAE drug-linker molecules are attached via their maleimides to two thiols in a Probody CX-151 replacing one interchain disulfide bond giving rise to the DPR = 2 species. Here only the most abundant DPR = 2 isomer of CX-2029 is depicted where a single light chain/heavy chain disulfide bond in one Fab arm is replaced by two vcMMAE molecules. Cleavage of the vc- linker upon PDC internalization releases the MMAE payload, which acts as an antimitotic drug via microtubule disruption. **B,** Anti-CD71 PDC (CX-2029) binding to CD71 is impaired by masking *in vitro*. **A, B,** Binding to recombinant human (**A**) and cynomolgus monkey (**B**) CD71 ECD was assessed using isotype control (black diamond), parental antibody CX-051 (green circle), anti-CD71 ADC CX-2030 (orange square), intact Probody therapeutic CX-151 (red triangle), matriptase-activated CX-151 (open red triangle), intact anti-CD71 PDC CX-2029 (solid blue triangle), and matriptase-activated anti-CD71 PDC CX-2029 (open blue triangle) as measured via indirect ELISA. Data points represent the mean of duplicate wells. Error bars show SEM. **C, D,** Binding to human breast cancer cell line HCC1806 (**C**) and cynomolgus monkey CD71-expressing CHO K1 cells (**D**) as measured by flow cytometry. Data points represent the median fluorescence intensity (MFI) and error bars reflect SEM.

a positive control. These data suggest that the parental antibody for the anti-CD71 PDC is a partial competitor with hTf for binding to human CD71.

Anti-CD71 PDC demonstrates broad, potent *in vivo* activity in preclinical xenograft models

The *in vivo* efficacy of the anti-CD71 PDC as an anticancer agent was examined in a wide variety of PDX tumor models (**Fig. 4**; Supplementary Fig. S4). PDX tumor-bearing mice were dosed with vehicle control (PBS), or 1.5, 3, or 6 mg/kg anti-CD71 PDC via i.v. injection on days 0 and 7 ($n = 3$ per group). PDX models included those representing gastric cancer, esophageal cancer, NSCLC, breast cancer, DLBCL, HNSCC, and pancreatic cancer. Among 34 PDX

models tested, 30 models expressed high levels of CD71, and four (one gastric, one pancreatic, and two esophageal) models expressed low levels of CD71.

As shown in **Fig. 4**, anti-CD71 PDC demonstrated significant tumor growth inhibition at 3 or 6 mg/kg in seven tumor models representing seven tumor indications tested. In most cases, this inhibition lasted for 60 days or longer at the 6 mg/kg dose level. In **Fig. 4** and Supplementary Fig. S4, tumor recurrence was observed at the 3 mg/kg dose level in several tumor lines starting at 40 days after initial treatment. The 1.5 mg/kg dose, which was tested in eight models, was ineffective in most models tested. Three of the four models that expressed low CD71 did not respond to the anti-CD71 PDC, suggesting that high target levels may be needed for anticancer activity, and consistent with
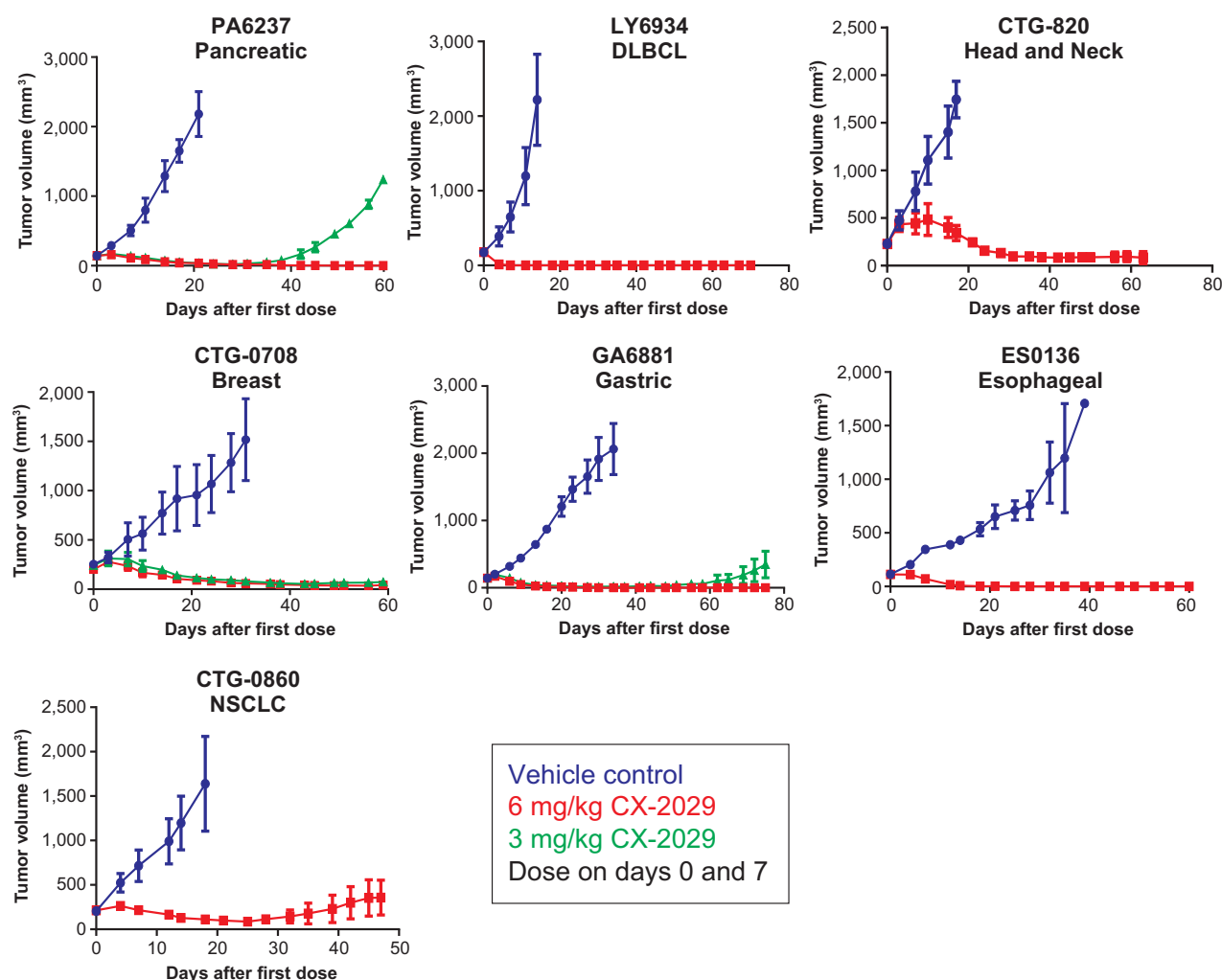
Figure 4.
Anti-CD71 PDC (CX-2029) inhibits tumor growth in PDX models across seven tumor indications. Animals harboring PDX tumors representing seven tumor indications (pancreatic, DLBCL, breast, gastric, esophageal, NSCLC, and HNSCC) were treated with vehicle or anti-CD71 PDC (CX-2029) at 3 or 6 mg/kg ($n = 3$ per group) on days 0 and 7 after randomization. Graphs depict average tumor volume over time with SEM.

the requirement of high target expression for ADC activity (20). Among the 34 PDX models tested at 3 or 6 mg/kg, 28 (82%) models responded with tumor regression or stasis.

In an additional study, an anti-CD71 ADC and PDC (both MMAE-conjugated, DAR~3) demonstrated comparable efficacy when evaluated in the HCC1806 xenograft tumor model (Supplementary Fig. S5). The anti-CD71 PDC used in this study differs from CX-2029 by a single amino acid change in the Probody. The data indicate that the Probody mask is effectively removed in the tumor microenvironment and does not impede efficacy. Collectively, the xenograft data indicate that the anti-CD71 PDC is a potent inhibitor of tumor growth across a wide variety of cancers and provide preclinical evidence of efficacy.

Pharmacokinetics of the anti-CD71 PDC in cynomolgus monkeys

The toxicokinetic profile of the anti-CD71 PDC was evaluated following i.v. administration to cynomolgus monkeys (**Fig. 5**; Supplementary Table S8). Four analytes were quantified to describe the toxicokinetics and activation state of the anti-CD71 PDC in cyno-

molgus monkey plasma; intact anti-CD71 PDC (referring to the masked, prodrug form), total anti-CD71 PDC (referring to the sum of intact and activated anti-CD71 PDC), Probody-conjugated MMAE (pc-MMAE), and nonconjugated MMAE (MMAE).

Dose-proportional exposure of the anti-CD71 PDC was observed across the dose range tested (2–12 mg/kg), based on C_{max} and AUC for the major analytes total anti-CD71 PDC, intact anti-CD71 PDC, and Probody therapeutic-conjugated (pc)-MMAE. Exposure values for total and intact anti-CD71 PDC were similar, suggesting limited activation of the Probody therapeutic in healthy tissues or in circulation. Deconjugation of the MMAE payload from the anti-CD71 PDC occurred over time, but the exposure of unconjugated MMAE was low at 12 mg/kg ($C_{max} < 0.13\%$ of the maximal pc-MMAE concentration) and not detectable at the 2 and 6 mg/kg dose levels.

Nonclinical safety of the anti-CD71 PDC and anti-CD71 ADC in cynomolgus monkeys

The cynomolgus monkey was identified as a pharmacologically relevant toxicity species for the anti-CD71 PDC based on the similar

Figure 5.
Mean plasma concentrations of intact and total anti-CD71 PDC, pc-MMAE, and MMAE in a cynomolgus monkey after a single i.v. dose. Cynomolgus monkeys were administered 2, 6, and 12 mg/kg anti-CD71 PDC (CX-2029), and plasma levels of (**A**) total CX-2029, and intact CX-2029 (where intact CX-2029 refers to the masked, prodrug form and total CX-2029 includes all circulating forms). (**B**) Probody therapeutic-conjugated (pc)-MMAE and nonconjugated MMAE were evaluated over time using validated HPLC/MS-MS methods. Figures show mean values with SD.
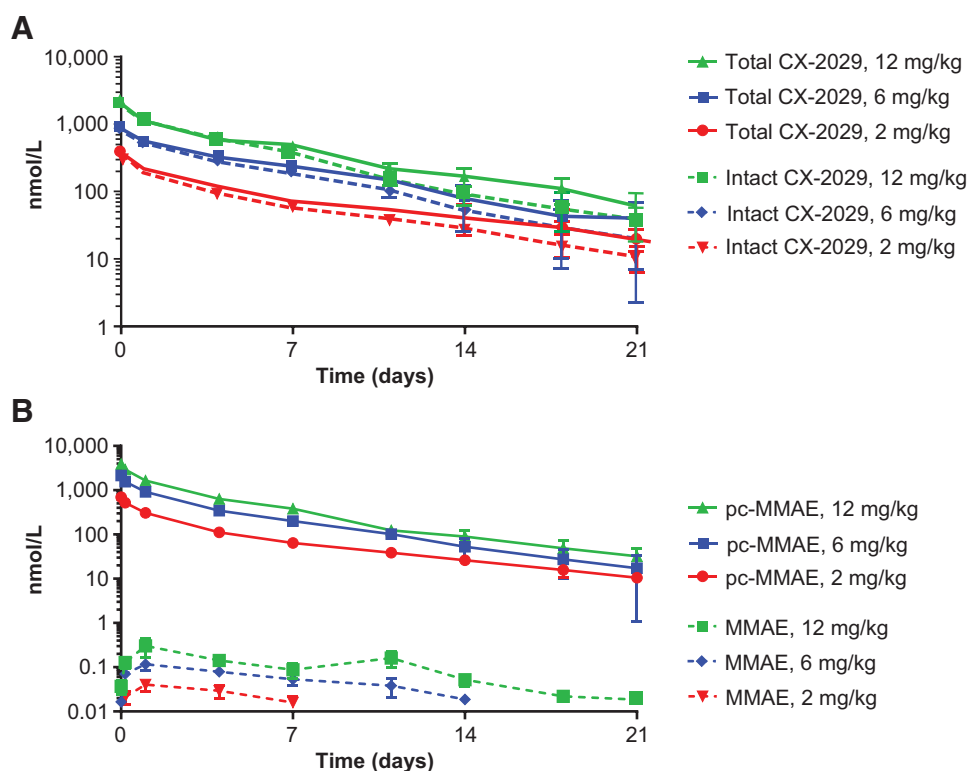
binding affinities of the parental antibody and activated PDC to human and monkey CD71, the similar concentrations of hTf (endogenous competitor for binding to CD71) in human and monkey serum (21), and the broad expression of CD71 in normal tissues of both species.

The relative safety of the anti-CD71 PDC and its nonmasked counterpart anti-CD71 ADC was evaluated in cynomolgus monkeys. The anti-CD71 ADC was tolerated as a repeat dose of 0.6 mg/kg administered on days 1 and 22, whereas the one animal receiving a single 2 mg/kg dose of this anti-CD71 ADC was found dead on day 9. The major and dose-limiting toxicity of anti-CD71 ADC was hematologic; findings included dose-dependent decreases in reticulocytes, red blood cell mass (red blood cell count, hemoglobin concentration, and hematocrit) and leukocytes, most notably neutrophils (**Fig. 6A**; Supplementary Fig. S6).

The tolerability of the anti-CD71 PDC was substantially higher than that of the anti-CD71 ADC, consistent with the expected reduction in binding to normal tissues. Repeat dosing of anti-CD71 PDC at 2 mg/kg was essentially a no-effect dose level. Anti-CD71 PDC-related changes in clinical pathology parameters at ≥ 6 mg/kg were generally dose-dependent and reversible. At 6 mg/kg, anti-CD71 PDC-related hematology findings were similar to those observed with anti-CD71 ADC at 0.6 mg/kg (**Fig. 6B**; Supplementary Fig. S6). Anti-CD71 PDC administration at 12 mg/kg resulted in a more profound reduction in neutrophil, reticulocyte, and hemoglobin levels, and three of 12 animals were either found dead or were euthanized on day 10 or 11. These deaths were attributed to septicemia based on microscopic evidence of bacterial infection that was considered secondary to immune suppression. Other animals in the 12 mg/kg dose group developed skin lesions consistent with infection. Also noted at 12 mg/kg were clinical chemistry indicators of acute phase response (decreased albumin and cholesterol; increased globulins, total bilirubin, and triglycerides). Most hematology findings recovered or rebounded by day 21, with the exception of a red blood cell

mass in the 12 mg/kg group, and all clinical pathology findings had reversed after a 6-week recovery phase. Microscopic changes noted at the terminal necropsy included bone marrow hypocellularity (erythroid and/or myeloid) at 6 mg/kg, decreased cellularity in the thymus at 6 and 12 mg/kg, and cortical hypertrophy in the adrenal gland at 12 mg/kg. Findings in animals that died early were similar to those observed at terminal necropsy with additional findings of decreased cellularity in spleen and mandibular and mesenteric lymph nodes. All findings were reversed in the recovery animals. The 10-fold improvement in tolerability of the anti-CD71 PDC compared with the unmasked anti-CD71 ADC is consistent with the expected attenuation of binding to CD71 in normal tissues.

Discussion

The goal of this series of studies was to assess the preclinical efficacy and safety of the anti-CD71 PDC CX-2029 and evaluate the potential for a PDC to successfully address a highly desirable but previously undruggable ADC target. The data presented here confirm that CD71 is a potentially attractive ADC target, with high membrane expression across a broad array of tumor indications. However, CD71 is also highly expressed in many normal tissues, necessitating a novel approach to specifically target the antigen in tumor tissues and create an acceptable therapeutic window. Using the Probody Therapeutic technology, masking of the target-binding epitope impaired binding of the anti-CD71 PDC to both human and cynomolgus CD71, and protease-mediated unmasking *in vitro* restored binding to levels seen with the native parental anti-CD71 antibody. The anti-CD71 PDC displayed potent inhibition of tumor growth across a broad range of PDX preclinical models. Furthermore, the tolerability of the anti-CD71 PDC in cynomolgus monkeys indicates substantially improved safety compared with the corresponding anti-CD71 ADC.
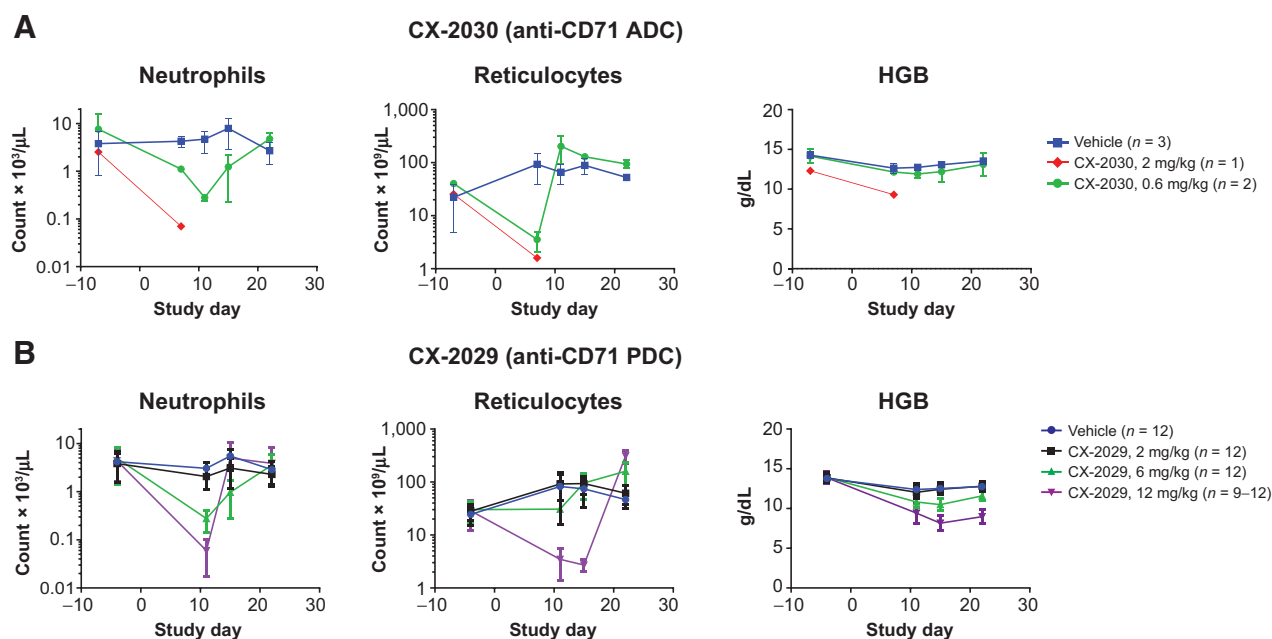
A

B

Figure 6.
Effects of anti-CD71 PDC and anti-CD71 ADC on hematology parameters in cynomolgus monkeys. Cynomolgus monkeys were administered 2 or 0.6 mg/kg of anti-CD71 ADC (CX-2030), and 2, 6, or 12 mg/kg of anti-CD71 PDC (CX-2029) by i.v. injection. Neutrophil count, reticulocyte count, and hemoglobin concentration (HGB) are shown for anti-CD71 ADC (**A**) and anti-CD71 PDC (**B**). Figures show mean values with SD.

Consistent with the results of this study, CD71 has previously been shown to be highly expressed in malignant tissues and may contribute to tumor progression in a variety of cancers including those that are sensitive to MTI drugs, such as esophageal, NHL (mostly DLBCL), lung, HNSCC, breast, ovarian, and endometrial cancers (9–12). In many cases, CD71 expression is many times higher in malignant cells than normal cells, and higher expression levels have been associated with advanced tumor stages or cancer progression (9, 10, 22–24). This elevated expression reflects the increased tumor demand for iron, which functions as a cofactor in many metabolic processes including DNA synthesis and cell proliferation. However, the data presented here and elsewhere have shown that CD71 is ubiquitously expressed in normal tissues, particularly rapidly proliferating cells, and is essential for erythropoiesis and hematopoiesis (25, 26). This expression and requirement of CD71 in normal tissues thus limits the potential therapeutic window achievable with an ADC approach.

Previous efforts to target CD71 or Tf using conjugated toxins have been unsuccessful in the clinic. The 454A12-RTA immunotoxin, in which a murine IgG1 targeting CD71 was conjugated to the catalytic subunit of the plant toxin ricin (RTA), was assessed for antitumor efficacy in two clinical trials. In one study of local treatment of metastatic intraperitoneal carcinoma with 454A12-RTA, no antitumor effects were observed, but systemic toxicity was reported, including a fatal encephalopathy with cerebral edema (13). In the second trial, local intraventricular 454A12-RTA treatment of patients with leptomeningeal systemic neoplasia resulted in reduced tumor cell counts in the cerebrospinal fluid with no systemic toxicity (27). Similarly, local treatment of patients with malignant brain tumors with Tf-CRM107, a conjugate of human Tf with diphtheria toxin that lacks native toxin binding (CRM107), resulted in a reduction in tumor volume in 60% of patients and peritumoral toxicity in 20% of patients (28). Despite previous efforts to deliver a wide variety of cytotoxic compounds, including chemotherapeutics, toxins, radio-isotopes, polymers, gene therapy vectors, and nanoparticles via targeting Tf or CD71, none have thus far shown an acceptable risk-benefit profile in clinical trials (29).

The PDC approach described here represents a promising strategy for leveraging the attractive properties of CD71 as an ADC target while limiting the on-target/off-tumor toxicities that have hampered previous efforts to drug this target. The data presented here demonstrate that the prodomain of the anti-CD71 PDC reduced binding to human CD71 by approximately 50-fold compared with the parental antibody and that protease activation restores full binding capacity. Because the PDC is designed to be activated by protease activities associated with tumor microenvironments, the binding of the anti-CD71 PDC to normal tissues should be limited, thereby enhancing the risk–benefit profile.

The parental antibody of the anti-CD71 PDC partially competes with hTF when binding to human CD71 (Supplementary Fig. S3). Given the profound toxicity observed with a low dose of the anti-CD71 ADC in cynomolgus monkeys, the competitive binding epitope of the parental antibody with hTF to CD71 may represent a favorable safety consideration.

In vivo, anti-CD71 PDC treatment resulted in potent tumor growth inhibition (stasis or regression) at 3 or 6 mg/kg dose levels in 28 of 34 PDX models tested, including seven different tumor types (pancreatic, gastric, esophageal, NSCLC, HNSCC, breast, and DLBCL). Most models expressed moderate to high levels of CD71. Three of four CD71 low-expressing models showed poor activity when treated with anti-CD71 PDC, consistent with the view that higher expressing tumors may respond better (20). The robust activity observed across multiple cancer types supports the potential for broad efficacy of the anti-CD71 PDC across multiple tumor indications in the clinic.

Dose-proportional exposure of the anti-CD71 PDC was observed over the 2 to 12 mg/kg dose range tested, and most anti-CD71 PDC in circulation was intact. Exposure of unconjugated MMAE was very low, suggesting stability of the vc linker and limited potential for toxicity due to circulating unconjugated MMAE.

Anti-CD71 PDC demonstrated a 10-fold improvement in tolerability compared with the DAR-2 purified anti-CD71 ADC, as seen by a right-shift in the dose–response curve for hematologic toxicity. MTDs for anti-CD71 PDC and anti-CD71 ADC were 6 and 0.6 mg/kg, respectively. Early deaths at doses exceeding the MTD for anti-CD71 PDC or anti-CD71 ADC were consistent with sepsis that was considered secondary to immune suppression. Toxicity findings for anti-CD71 PDC, which included dose-dependent decreases in red blood cell mass, reticulocytes, and all leukocyte subsets, were generally consistent with publicly available cynomolgus toxicity data for other MMAE ADCs (30, 31) and were largely reversed within 3 weeks after dosing.

Together, these studies demonstrate potential of the PDC approach to target otherwise "undruggable" tumor antigens and provide a sound scientific basis for the development of this anti-CD71 PDC as a novel therapeutic for the treatment of cancer. CX-2029 is now being investigated in a phase I/II clinical trial in patients with metastatic or locally advanced unresectable solid tumors or DLBCL.

Authors' Disclosures

S. Singh reports multiple pending and issued patents. L. Serwer reports other support from CytomX Therapeutics during the conduct of the study, as well as other support from CytomX Therapeutics outside the submitted work. K. Elkins reports multiple pending patent applications. N. Chauhan reports AbbVie, Inc. has a collaboration and license deal with CytomX for the compounds in question. L. Wang reports employment with AbbVie, Inc. K. Tipton reports a patent for US10179817B2 issued to CytomX Assignee. I. Badagnani reports a patent for WO 2019/075417 (Anti-CD71 activatable antibody drug conjugates and methods of use thereof) pending. S. Jeffries reports employment with AbbVie, Inc. R. Leanna reports multiple pending patent applications. L. Desnoyers reports other support from CytomX Therapeutics and CytomX Therapeutics outside the submitted work; also has patent 10,179,817 issued, patent 20190202927 pending, and patent 20160355599 pending. J. Terrett reports a patent for CN-108026170-A pending. S. Morgan-Lappe reports a patent for Anti-CD71 activatable antibody–drug conjugates and methods of use thereof pending; and AbbVie, Inc. has a codevelopment license deal with CytomX for CX-2029. W.M. Kavanaugh reports other support from AbbVie Inc. during the conduct of the study; also reports multiple pending and issued patents and reports employment with CytomX Therapeutics, Inc. and ownership of CytomX Therapeutics, Inc. stock.

J. Richardson reports a patent for One pending. No disclosures were reported by the other authors.

Authors' Contribution

S. Singh: Conceptualization, resources, formal analysis, methodology, writing–original draft, writing–review and editing. L. Serwer: Methodology, writing–review and editing. A. DuPage: Methodology, writing–review and editing. K. Elkins: Methodology, writing–review and editing. N. Chauhan: Methodology, writing–review and editing. M. Ravn: Methodology, writing–review and editing. F. Buchanan: Methodology, writing–review and editing. L. Wang: Methodology, writing–review and editing. M. Krimm: Methodology, writing–review and editing. K. Wong: Methodology, writing–review and editing. J. Sagert: Methodology, writing–review and editing. K. Tipton: Methodology, writing–review and editing. S.J. Moore: Methodology, writing–review and editing. Y. Huang: Methodology, writing–review and editing. A. Jang: Methodology, writing–review and editing. E. Ureno: Methodology, writing–review and editing. A. Miller: Methodology, writing–review and editing. S. Patrick: Methodology, writing–review and editing. S. Duvur: Methodology, writing–review and editing. S. Liu: Methodology, writing–review and editing. O. Vasiljeva: Methodology, writing–review and editing. Y. Li: Methodology, writing–review and editing. T. Henriques: Methodology, writing–review and editing. I. Badagnani: Methodology, writing–review and editing. S. Jeffries: Methodology, writing–review and editing. S. Schleyer: Methodology, writing–review and editing. R. Leanna: Methodology, writing–review and editing. C. Krebber: Methodology, writing–review and editing. S. Viswanathan: Methodology, writing–review and editing. L. Desnoyers: Methodology, writing–review and editing. J. Terrett: Methodology, writing–review and editing. M. Belvin: Conceptualization, methodology, writing–original draft, writing–review and editing. S. Morgan-Lappe: Methodology, writing–review and editing. W.M. Kavanaugh: Conceptualization, methodology, writing–review and editing. J. Richardson: Conceptualization, resources, supervision, validation, methodology, writing–original draft, project administration, writing–review and editing.

Acknowledgments

Note

Supplementary data for this article are available at Molecular Cancer Therapeutics Online (http://mct.aacrjournals.org/).

References

1. U.S. Food and Drug Administration. Hematology/Oncology (Cancer) Approvals & Safety Notifications. October 26, 2020. https://www.fda.gov/drugs/resources-information-approved-drugs/hematologyoncology-cancer-approvals-safety-notifications. Accessed November 5, 2020.
2. Joubert N, Beck A, Dumontet C, Denevault-Sabourin C. Antibody-drug conjugates: the last decade. Pharmaceuticals 2020;13:245.
3. Ponziani S, Di Vittorio G, Pitari G, Cimini AM, Ardini M, Gentile R, et al. Antibody-drug conjugates: the new frontier of chemotherapy. Int J Mol Sci 2020;21:5510.
4. Francisco JA, Cerveny CG, Meyer DL, Mixan BJ, Klussman K, Chace DF, et al. cAC10-vcMMAE, an anti-CD30-monomethyl auristatin E conjugate with potent and selective antitumor activity. Blood 2003;102:1458–65.
5. Beck A, Goetsch L, Dumontet C, Corvaïa N. Strategies and challenges for the next generation of antibody-drug conjugates. Nat Rev Drug Discov 2017;16:315–37.
6. de Goeij BE, Lambert JM. New developments for antibody-drug conjugate-based therapeutic approaches. Curr Opin Immunol 2016;40:14–23.
7. Ab O, Whiteman KR, Bartle LM, Sun X, Singh R, Tavares D, et al. IMGN853, a folate receptor-α (FRα)-targeting antibody-drug conjugate, exhibits potent targeted antitumor activity against FRα-expressing tumors. Mol Cancer Ther 2015;14:1605–13.
8. Trowbridge IS, Domingo DL. Anti-transferrin receptor monoclonal antibody and toxin-antibody conjugates affect growth of human tumour cells. Nature 1981;294:171–3.
9. Habeshaw JA, Lister TA, Stansfeld AG, Greaves MF. Correlation of transferrin receptor expression with histological class and outcome in non-Hodgkin lymphoma. Lancet 1983;1:498–501.
10. Kondo K, Noguchi M, Mukai K, Matsuno Y, Sato Y, Shimosato Y, et al. Transferrin receptor expression in adenocarcinoma of the lung as a histopathologic indicator of prognosis. Chest 1990;97:1367–71.
11. Habashy H, Powe D, Staka C, Rakha EA, Ball G, Green AR, et al. Transferrin receptor (CD71) is a marker of poor prognosis in breast cancer and can predict response to tamoxifen. Breast Cancer Res Treat 2010;119:283–93.
12. Chan K, Choi M, Lai K, Tan W, Tung LN, Lam HY, et al. Overexpression of transferrin receptor CD71 and its tumorigenic properties in esophageal squamous cell carcinoma. Oncol Rep 2014;31:1296–304.
13. Ghetie V, Vitetta E. Immunotoxins in the therapy of cancer: from bench to clinic. Pharmacol Ther 1994;63:209–34.

14. Desnoyers LR, Vasiljeva O, Richardson JH, Yang A, Menendez EE, Liang TW, et al. Tumor-specific activation of an EGFR-targeting probody enhances therapeutic index. Sci Transl Med 2013;5:207ra144.

15. Autio KA, Boni V, Humphrey RW, Naing A. Probody therapeutics: An emerging class of therapies designed to enhance On-target effects with reduced Off-tumor toxicity for use in Immuno-oncology. Clin Cancer Res 2020;26:984–9.

16. Kavanaugh WM. Antibody prodrugs for cancer. Expert Opin Biol Ther 2020;20: 163–71.

17. Vasiljeva O, Hostetter DR, Moore SJ, Winter MB. The multifaceted roles of Tumor-associated proteases and harnessing their activity for prodrug activation. Biol Chem 2019;400:965–77.

18. Boni V, Burris III HA, Liu JF, Spira AI, Arkenau H-T, Fidler MJ, et al. CX-2009, a CD166-directed probody drug conjugate (PDC): Results from the first-in-human study in patients (Pts) with advanced cancer including breast cancer (BC). J Clin Oncol 38:15s, 2020 (suppl abstr 526).

19. Singh S, Richardson JH, Serwer LP, Terrett JA, Morgan-Lappe SE, Henriques T, et al., Inventors. Anti-CD71 activatable antibody drug conjugates and methods of use thereof. AbbVie Inc., North Chicago, IL. U.S. patent publication no. US 2019/0111150 A1. Published April 18, 2019.

20. Lambert JM, Morris CQ. Antibody-drug conjugates (ADCs) for personalized treatment of solid tumors: a review. Adv Ther 2017;34:1015–35.

21. Giulietti M, La Torre R, Pace M, Iale E, Patella A, Turillazzi P. Reference blood values of iron metabolism in cynomolgus macaques. Lab Anim Sci 1991; 41:606–8.

22. Yang DC, Wang F, Elliott RL, Head JF. Expression of transferrin receptor and ferritin H-chain mRNA are associated with clinical and histopathological prognostic indicators in breast cancer. Anticancer Res 2001;21:541–9.

23. Prior R, Reifenberger G, Wechsler W. Transferrin receptor expression in tumours of the human nervous system: relation to tumour type, grading and tumour growth fraction. Virchows Arch A Pathol Anat Histopathol 1990;416: 491–6.

24. Gupta AD, Shah VI. Correlation of transferrin receptor expression with histologic grade and immunophenotype in chronic lymphocytic leukemia and non-Hodgkin's lymphoma. Hematol Pathol 1990;4:37–41.

25. Levy JE, Jin O, Fujiwara Y, Kuo F, Andrews NC. Transferrin receptor is necessary for development of erythrocytes and the nervous system. Nat Genet 1999;21: 396–9.

26. Wang S, He X, Wu Q, Jiang L, Chen L, Yu Y, et al. Transferrin receptor 1-mediated iron uptake plays an essential role in hematopoiesis. Haematologica 2020;105:2071–82.

27. Laske DW, Muraszko KM, Oldfield EH, DeVroom HL, Sung C, Dedrick RL, et al. Intraventricular immunotoxin therapy for leptomeningeal neoplasia. Neurosurgery 1997;41:1039–49.

28. Laske DW, Youle RJ, Oldfield EH. Tumor regression with regional distribution of the targeted toxin TF-CRM107 in patients with malignant brain tumors. Nat Med 1997;3:1362–8.

29. Daniels TR, Bernabeu E, Rodríguez JA, Patel S, Kozman M, Chiappetta DA, et al. The transferrin receptor and the targeted delivery of therapeutic agents against cancer. Biochim Biophys Acta 2012;1820:291–317.

30. Saber H, Leighton JK. An FDA oncology analysis of antibody-drug conjugates. Regul Toxicol Pharmacol 2015;71:444–52.

31. Li D, Lee D, Dere RC, Zheng B, Yu SF, Fuh FK, et al. Evaluation and use of an anti-cynomolgus monkey CD79b surrogate antibody-drug conjugate to enable clinical development of polatuzumab vedotin. Br J Pharmacol 2019;176: 3805–18.